Polymer Chemistry

RSCPublishing

ARTICLE

$B(C_6F_5)_3$-Catalyzed Group Transfer Polymerization of Alkyl Methacrylates with Dimethylphenylsilane through *in Situ* Formation of Silyl Ketene Acetal by $B(C_6F_5)_3$-Catalyzed 1,4-Hydrosilylation of Methacrylate Monomer

Cite this: DOI: 10.1039/x0xx00000x

Received 00th January 2015,
Accepted 00th January 2015,

DOI: 10.1039/x0xx00000x

www.rsc.org/

*Yougen Chen,[§,¶] Kodai Kitano,[‡,¶] Shinji Tsuchida,[‡] Seiya Kikuchi,[‡] Kenji Takada,[‡] Toshifumi Satoh,[‡†] and Toyoji Kakuchi[§‡†]**

The group transfer polymerization (GTP) of alkyl methacrylates has been studied using hydrosilane and tris(pentafluorophenyl)borane ($B(C_6F_5)_3$) as the new initiation system. For the $B(C_6F_5)_3$-catalyzed polymerization of methyl methacrylate (MMA) using triethylsilane, tri-*n*-butylsilane ($n$$Bu_3SiH$), dimethylphenylsilane (Me_2PhSiH), triphenylsilane, and triisopropylsilane, $n$$Bu_3SiH$ and Me_2PhSiH were suitable for producing well-defined polymers with predicted molar masses and a low polydispersity. The livingness of the GTP of MMA using $Me_2PhSiH/B(C_6F_5)_3$ was verified by the matrix-assisted laser desorption/ionization time-of-flight mass spectrometry (MALDI-TOF MS) measurement of the resulting polymers, kinetic analyses, and chain extension experiments. The $B(C_6F_5)_3$-catalyzed GTP using Me_2PhSiH was also applicable for other alkyl methacrylates, such as the *n*-propyl, *n*-hexyl, *n*-decyl, 2-ethylhexyl, *iso*-butyl, and cyclohexyl methacrylates. The *in situ* formation of the silyl ketene acetal by the 1,4-hydrosilylation of MMA was proved by the MALDI-TOF MS and ^2H NMR measurements of the polymers obtained from the $B(C_6F_5)_3$-catalyzed GTPs of MMA with Me_2PhSiH or Me_2PhSiD, which was terminated using CH_3OH or CD_3OD.

Introduction

Group transfer polymerization (GTP) using a silyl ketene acetal (SKA) is categorized as an anionic polymerization method, which has been utilized for polar vinyl monomers, such as alkyl (meth)acrylates and *N*,*N*-dialkylacrylamides. In principle, the initiation and propagation reactions during the GTP process are rooted in the Mukaiyama-Michael reaction,[1-3] and both a Lewis base and Lewis acid are used as catalysts for the GTP as well as the Mukaiyama-Michael reaction. Although conventional catalysts of Lewis bases, such as nucleophilic anions of $SiMe_3F_2^-$,[1,4,5] HF_2^-,[1,4-6] and CN^-,[1,4,6,7] and Lewis acids, such as the transition metal compounds of ZnX_2 (X = Cl, Br, and I) [6,8] were used for the polymerization of (meth)acrylate monomers, they usually needed to be optimized in light of the reactivity of the used monomers. Basically, the controlled GTP of methacrylate monomers had been achieved using conventional nucleophilic anions, while the GTP of acrylate monomers was hardly controlled. On the other hand, organocatalysts have been applied to various GTP systems, resulting in achieving significant improvements of their controlled/living characteristics by the suppression of side reactions, such as transfer reactions to monomers and polymers, due to the low nucleophilicity of the base organocatalysts and the strong Lewis acidity of the acid ones.[9] Thus, base organocatalysts, such as *N*-heterocyclic carbene (NHC),[10-13] 2,8,9-triisobutyl-2,5,8,9-tetraaza-1-phosphabicyclo[3.3.3]undecane,[14] 1-*tert*-butyl-4,4,4-tris(dimethylamino)-2,2-bis[tris(dimethylamino)-phosphoranylidenamino]-2Λ^5,4Λ^5-catenadi(phosphazene),[14-16] and tris(2,4,6-trimethoxyphenyl)phosphine,[17] have been used for the controlled/living GTPs of methyl methacrylate (MMA) and *tert*-butyl acrylate. In addition, acid organocatalysts, such as triphenylmethyl tetrakis(pentafluorophenyl)borane,[18-21] (*R*)-3,3'-bis[3,5-bis(trifluoromethyl)phenyl]-1,1'-binaphthyl-2,2'-disulfonimide,[22] trifluoromethanesulfonimide,[23-26] *N*-(trimethylsilyl)triflylimide,[27,28] and 1-[bis(trifluoromethanesulfonyl)methyl]-2,3,4,5,6-pentafluorobenzene,[25,26] were suitable for the controlled/living GTPs of methacrylate, acrylate, and acrylamide monomers, α-methylene-γ-butyrolactone, and γ-methyl-α-methylene-γ-butyrolactone using the appropriate SKAs as initiators. Furthermore, we reported that the acid organocatalysts have been used to synthesize well-defined and structurally defect-free end-functionalized poly(methyl methacrylate)s (PMMAs) and poly(*n*-butyl acrylate)s in our recent reports.[29,30]

The challenging tasks in the GTP chemistry are related to the development of versatile catalysts for the random and block copolymerizations of different types of monomers and the use of an

unstable SKA. For the former issue, Taton et al. reported that NHC was efficient for the synthesis of block copolymers composed of methacrylate and acrylate monomers, *N*,*N*-dimethylacrlamide, and methacrylonitrile.[12,13] For the latter issue, we recently reported the polymerization of *n*-butyl acrylate (*n*BA) by combining the use of hydrosilane (R_3SiH) and tris(pentafluorophenyl)borane ($B(C_6F_5)_3$) as a novel and very convenient GTP method without the direct use of the unstable SKA, in which the true initiator of (*Z*)-1-*n*-butoxy-1-dimethylphenylsiloxy-1-propene *in situ* formed as fast as a propagation reaction, proceeded through the 1,4-hydrosilylation of *n*BA with the moisture-stable R_3SiH of dimethylphenylsilane.[31] Thus, it is interesting to clarify the limit and scope of this GTP method, such as the applicable monomers and a suitable combination of R_3SiH with the used monomer. In this study, we now report the GTP of methacrylate monomers, whose reactivity significantly differs from acrylate monomers for the anionic polymerizations involving the GTP using R_3SiH and $B(C_6F_5)_3$. This article describes (1) the GTP of MMA using R_3SiH and $B(C_6F_5)_3$ in terms of the optimization of R_3SiH, kinetic studies, and molar-mass control, (2) the structural effect of the methacrylate monomers on this GTP characteristcs, and (3) the mechanism investigations based on the *in situ* 1,4-hydrosilylation of MMA with Me_2PhSiH or Me_2PhSiD, which was terminated using CH_3OH or CD_3OD.

Scheme 1. $B(C_6F_5)_3$-catalyzed group transfer polymerizations (GTP) of methacrylate monomers using Me_2PhSiH.

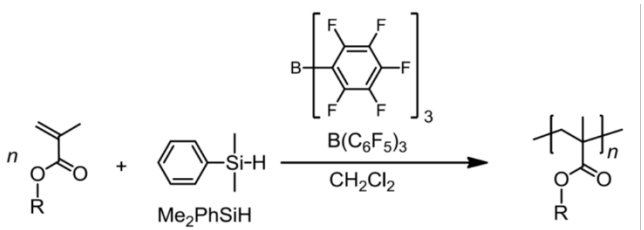

R	Monomer	Polymer
CH_3	MMA	PMMA
$CH_2CH_2CH_3$	*n*PrMA	P*n*PrMA
$CH_2(CH_2)_4CH_3$	*n*HMA	P*n*HMA
$CH_2(CH_2)_8CH_3$	*n*DMA	P*n*DMA
$CH_2CH(CH_2CH_3)C_4H_9$	EHMA	PEHMA
$CH_2CH(CH_3)_2$	*i*BuMA	P*i*BuMA
cyclo-C_6H_{11}	CyHMA	P*c*HMA
$C(CH_3)_3$	*t*BuMA	P*t*BuMA
$CH_2CH{=}CH_2$	AMA	PAMA
$CH_2CH_2OCH_2CH_2OCH_3$	DEGMA	PDEGMA

Experimental Section

Materials. Dichloromethane (CH_2Cl_2, >99.5%; water content, <0.001%), *n*-butyllithium (*n*BuLi, 1.6 mol L^{-1} in *n*-hexane), triethylamine (>99.0%), calcium hydride (CaH_2, >95.0%), methanol (>99.5%), *n*-hexane (>95.0%), and deuterated chloroform ($CDCl_3$, >99.8%) were purchased from Kanto Chemicals Co., Inc. Methyl methacrylate (MMA, >99.8%), *n*-propyl methacrylate (*n*PrMA, >98.0%), isobutyl methacrylate (*i*BuMA, >98.0%), *n*-hexyl methacrylate (*n*HMA, >98.0%), 2-ethylhexyl methacrylate (EHMA, >99.0%), cyclohexyl methacrylate (*c*HMA, >98.0%), *n*-dodecyl methacrylate (*n*DMA, >95.0%), *tert*-butyl methacrylate (*t*BuMA, >98.0%), allyl methacrylate (AMA, >99.0%), 2-(2-methoxyethoxy)ethyl methacrylate (DEGMA, >97.0%), *trans*-3-indoleacrylic acid (>98.0%), triethylsilane (Et_3SiH, >98.0%), tri-*n*-butylsilane (nBu_3SiH, >98.0%), triisopropylsilane (iPr_3SiH, >98.0%), dimethylphenylsilane (Me_2PhSiH, >97.0%), triphenylsilane (Ph_3SiH, >96.0%), and methyl isobutyrate (>99.0%) were purchased from Tokyo Kasei Kogyo Co., Ltd. Tris(pentafluorophenyl)borane ($B(C_6F_5)_3$, >96.0%) was purchased from Wako Pure Chemicals Industries, Ltd., and used after recrystallization in *n*-hexane at −30 °C. Dithranol (>90.0%), silver trifluoroacetate (98.0%), sodium trifluoroacetate (98.0%), and deuterated methanol (CD_3OD, > 99.8%) were purchased from the Sigma-Aldrich Chemicals Co. MMA, *n*PrMA, *i*BuMA, *n*HMA, EHMA, *c*HMA, *n*DMA, *t*BuMA, AMA, DEGMA, CH_2Cl_2, Et_3SiH, $(nBu)_3SiH$, iPr_3SiH, Me_2PhSiH, and methyl isobutyrate were distilled from CaH_2 and degassed by three freeze-pump-thaw cycles prior to use. Ph_3SiH was recrystallized from *n*-hexane prior to use. 1-Methoxy-2-methyl-1-dimethylphenylsiloxyprop-1-ene (SKA^{Me_2Ph}) and deterodimethylphenylsilane (Me_2PhSiD) were synthesized according to previously reported procedures.[29,32] All other chemicals were purchased from available suppliers and used without further purification.

Measurements. The ^1H (400 MHz) and ^{13}C NMR (100 MHz) spectra were recorded using a JEOL JNM-A400II or a JEOL-ECS400. The ^2H NMR (61.4 MHz) spectra were recorded using a JEOL JNM-ECX400P. The polymerization solution was prepared in an MBRAUN stainless steel glove-box equipped with a gas purification system (molecular sieves and copper catalyst) in a dry argon atmosphere (H_2O, O_2 <1 ppm). The moisture and oxygen contents in the glove-box were monitored by an MB-MO-SE 1 and an MB-OX-SE 1, respectively. Size exclusion chromatography (SEC) measurements of the PMMAs were performed at 40 °C using a Jasco GPC-900 system (Shodex® DU-2130 dual pump, Shodex® RI-71 RI detector, and Shodex® ERC-3125SN degasser) equipped with two Shodex KF-804 L columns (linear, 8 mm × 300 mm) in THF at the flow rate of 1.0 mL min^{-1}. The number average molar mass ($M_{n,SEC}$) and dispersity (M_w/M_n) of the resulting PMMA were determined based on PMMA standards with the M_ws (M_w/M_ns) of 1.25×10^6 g mol^{-1} (1.07), 6.59×10^5 g mol^{-1} (1.02), 3.003×10^5 g mol^{-1} (1.02), 1.385×10^5 g mol^{-1} (1.05), 6.015×10^4 g mol^{-1} (1.03), 3.053×10^4 g mol^{-1} (1.02), and 1.155×10^4 g mol^{-1} (1.04), 4.90×10^3 g mol^{-1} (1.10), 2.87×10^3 g mol^{-1} (1.06), and 1.43×10^3 g mol^{-1} (1.15). The matrix-assisted laser desorption/ionization time-of-flight mass spectrometry (MALDI-TOF MS) measurements were performed using an Applied Biosystems Voyager-DE STR-H mass spectrometer with a 25 kV acceleration voltage. The positive ions were detected in the reflector mode (25 kV). A nitrogen laser (337 nm, 3 ns pulse width, 106-107 W cm^{-2}) operating at 3 Hz was used to produce the laser desorption, and 200-500 shots were summed. The spectra were externally calibrated using narrow-dispersed polystyrene with a linear calibration. Samples for the MALDI-TOF MS

measurements for the PMMAs were prepared by mixing the polymer (1.5 mg mL^{-1}, 10 μL), the matrix (trans-3-indoleacrylic acid, 10 mg mL^{-1}, 90 μL), and the cationizing agent (sodium trifluoroacetate, 10 mg mL^{-1}, 10 μL) in THF.

Synthesis of 1-methoxy-2-methyl-1-dimethylphenylsiloxyprop-1-ene (SKA^{Me_2Ph}). To a solution of diisopropylamine (3.09 mL, 22.0 mmol) in dry THF (50 mL) in a 100-mL cock-attached flask, *n*-butyllithium (13.8 mL, 22.0 mmol; 1.62 mol L^{-1} in *n*-hexane) was dropwise added for several minutes at 0 °C under an argon atmosphere. After stirring for 30 min, methyl isobutyrate (2.27 g, 22.0 mmol) was slowly added. After the reaction mixture was stirred at −78 °C for 30 min, phenyldimethylchlorosilane (3.70 mL, 22.0 mmol) was added. The entire mixture was warmed to room temperature and stirred overnight. The solvent was removed under reduced pressure, and the residue was distilled (54 °C, 0.02 mmHg) to give SKA^{Me_2Ph} as a colorless liquid. Yield, 620 mg (13.1 %). ^{1}H NMR (400 MHz, $CDCl_3$,): δ (ppm) 7.69-7.31 (m, 5H, -C_6H_5), 3.41 (s, 3H, -OCH_3), 1.61-1.47 (s, 6H, -$C(CH_3)_2$), 0.63 (s, 6H, -$Si(CH_3)_2C_6H_5$). ^{13}C NMR (100 MHz, $CDCl_3$,): δ (ppm) -1.31 (2C, -$Si(CH_3)_2C_6H_5$), 16.1-17.2 (2C, =$C(CH_3)_2$), 57.1 (1C, $COCH_3$), 91.6 (1C, C=$C(CH_3)_2$), 127.45-137.45 (6C, $OSi(CH_3)_2C_6H_5$), 149.54 (1C, C=$COCH_3$).

$B(C_6F_5)_3$-Catalyzed GTP of MMA using hydrosilane. A typical procedure is as follows: a stock solution of $B(C_6F_5)_3$ (250 μL, 12.5 μmol, 0.05 mol L^{-1} in CH_2Cl_2) was added to a solution of MMA (63.0 mg, 0.625 mmol) and Me_2PhSiH (3.83μL, 25.0 μmol) in CH_2Cl_2 (304 μL) under an argon atmosphere at room temperature. After stirring for 45 min, the polymerization was quenched by adding a small amount of methanol. Aliquots were removed from the reaction mixture to determine the conversion of MMA based on its ^{1}H NMR spectrum. The reaction mixture was purified by reprecipitation from CH_2Cl_2 into *n*-hexane, and dried in vacuo to give the PMMA as a white solid. Yield, 50.0 mg (80%). $M_{n,SEC}$, 3.20 kg mol^{-1} and M_w/M_n, 1.09.

Results and discussion

Group transfer polymerization of MMA using $B(C_6F_5)_3$ and R_3SiH. All the polymerizations of methyl methacrylate (MMA) were performed in CH_2Cl_2 at room temperature using tris(pentafluorophenyl)borane ($B(C_6F_5)_3$) as the catalyst. Initially, five hydrosilanes (R_3SiH), such as triethylsilane (Et_3SiH), tri-*n*-butylsilane (nBu_3SiH), dimethylphenylsilane (Me_2PhSiH), triphenylsilane (Ph_3SiH), and triisopropylsilane (iPr_3SiH), were used at the $[MMA]_0/[R_3SiH]_0/[B(C_6F_5)_3]_0$ ratio of 25/1/0.5 to assess the effect of the R_3SiH structure on the group transfer polymerization (GTP) characteristics of MMA. Table 1 summarizes the polymerization results. The required polymerization time for a complete monomer conversion increased with the increasing bulkiness of R_3SiH in the order of Et_3SiH < nBu_3SiH < Me_2PhSiH < Ph_3SiH < iPr_3SiH, such as 0.5, 0.5, 0.75, 1.65, and 115 h for Et_3SiH, nBu_3SiH, Me_2PhSiH, Ph_3SiH, and iPr_3SiH, respectively, indicating that the bulkiness of R_3SiH had a significant influence on the 1,4-hydrosilylation and propagation rates. The balance of these two rates turned out to be crucially important for the molar mass control. For instance, the polymerizations using nBu_3SiH and Me_2PhSiH as moderately bulky R_3SiHs produced poly(methyl methacrylate)s (PMMAs, runs 2 and 3, respectively) with the measured molar masses ($M_{n,SEC}$) of 3.4 and 3.2 kg mol^{-1} and the low polydispersities of 1.11 and 1.09, respectively, even though Me_2PhSiH was slightly better than nBu_3SiH in controlling the molar mass and polydispersity. Although their $M_{n,SEC}$s differed from the calculated molar mass ($M_{n,calcd.}$) of 2.5 kg mol^{-1} due to the limitation of the SEC measurement using PMMA standards, they agreed with the molar mass estimated by the matrix-assisted laser desorption/ionization time-of-flight mass spectrometry (MALDI-TOF MS) measurements. nBu_3SiH and Me_2PhSiH are considered to have the appropriate bulkiness to balance the 1,4-hydrosilylation rate (k_h) and the propagation rate (k_p) in the polymerization. In contrast, the polymerizations using Et_3SiH (run 1) or Ph_3SiH (run 4) and iPr_3SiH (run 5) as less or more bulky R_3SiHs, respectively, did not show molar-mass control even though the polydispersities of $\leqq 1.23$ were obtained. The kinetic studies were carried out in CH_2Cl_2 at room temperature using Et_3SiH, nBu_3SiH, Me_2PhSiH, Ph_3SiH, and iPr_3SiH at the $[MMA]_0/[R_3SiH]_0/[B(C_6F_5)_3]_0$ ratio of 50/1/0.5 to compare their polymerization characteristics, as shown in Figure 1, and the propagation rate (k_p) during the early polymerization stage and the induction period time (t_i) are summarized in Table 2. The polymerization using Et_3SiH led to a very fast propagation as the k_p of 0.1501 min^{-1} during the early polymerization period, which was three times greater than those using nBu_3SiH (0.0519 min^{-1}) and Me_2PhSiH (0.0494 min^{-1}). Given that Et_3SiH has a bulky structure similar to that of nBu_3SiH, their k_hs are assumed to be comparable though the k_h value was actually unable to be determined due to the extremely fast completion of the 1,4-hydrosilylation. Thus, the extremely high k_p for the polymerization using Et_3SiH eventually resulted in the higher molar mass (the $M_{n,SEC}$ of 5.6 kg mol^{-1}) than the predicted one (the $M_{n,calcd.}$ of 2.5 kg mol^{-1}). The reason why the polymerization using Ph_3SiH afforded the PMMA with the $M_{n,SEC}$ of 1.1 kg mol^{-1} is lower than the targeted molar mass of 2.5 kg mol^{-1} is still unclear. For the polymerization using the fairly bulky iPr_3SiH, a very long time of 115 h to complete the polymerization was required, and the $M_{n,SEC}$ of 10.0 kg mol^{-1} for the obtained PMMA was much higher than the targeted molar mass of 2.5 kg mol^{-1}. This result suggested a very low initiation efficiency, which was caused by the very slow reaction rate of the 1,4-hydrosilylation of MMA with iPr_3SiH and/or the Mukaiyama-Michael reaction of MMA with the *in situ* formed SKA. Although the effect of the R_3SiH structure on the polymerization control needs to be further investigated, we determined Me_2PhSiH to be the most suitable hydrosilane for the controlled GTP of MMA using the $B(C_6F_5)_3$ catalyst.

The MALDI-TOF MS measurement was implemented using a low molar-mass PMMA with the average degree of polymerization of ca. 50 to elucidate the compositional structure of the resulting PMMA. As shown in Figure S1, only one population of molecular ion peaks was observed and the interval between any two neighboring molecular ion peaks was ca. 100.05 Da, which was in

good agreement with the exact molar mass of MMA as the repeating unit (M.W. = 100.05). In addition, the observed *m/z* value of a specified 50-mer molecular ion peak at 5030.52 Da was extremely close to the calculated molar mass of 5030.80 Da for the polymer with a sodium-cationized 50-mer structure of [H-(MMA)$_{50}$-H + Na]$^+$.

Table 1. $B(C_6F_5)_3$-catalyzed GTP of MMA using hydrosilane (R_3SiH) as a potential initiator [a]

run	R_3SiH	Time (h)	$M_{n,SEC}$ [b] (kg mol^{-1})	M_w/M_n [b]
1	Et_3SiH	0.50	5.6	1.06
2	nBu_3SiH	0.50	3.4	1.11
3	Me_2PhSiH	0.75	3.2	1.09
4	Ph_3SiH	1.65	1.1	1.23
5	iPr_3SiH	115	10.0	1.17

[a] Solvent, CH_2Cl_2; temperature, r.t.; Ar atmosphere; $[MMA]_0$, 1.0 mol L^{-1}; $[MMA]_0/[R_3SiH]_0/[B(C_6F_5)_3]_0$, 25/1/0.5; MMA conversion (conv.) determined by ^{1}H NMR in $CDCl_3$, >99 %; $M_{n,calcd}$ (calculated by $[MMA]_0/[R_3SiH]_0 \times$ (conv.) $\times$ (M.W. of MMA) + (M.W. of H) $\times$ 2), 2.5 kg mol^{-1}. [b] Determined by SEC in THF using PMMA standards.

Table 2. The propagation rate of polymerization (k_p) during the early polymerization stage and the induction period time (t_i) for the $B(C_6F_5)_3$-catalyzed GTPs of MMA using various hydrosilanes [a]

Hydrosilane (Monomer)	k_p (min^{-1})	t_i (min)
Et_3SiH	0.1501	6.6
nBu_3SiH	0.0519	0
Me_2PhSiH	0.0498	6.3
Ph_3SiH	0.0302	8.2

[a] Solvent, CH_2Cl_2; temperature, r.t.; Ar atmosphere; $[MMA]_0$, 1.0 mol L^{-1}; $[MMA]_0/[R_3SiH]_0/[B(C_6F_5)_3]_0$, 50/1/0.5.

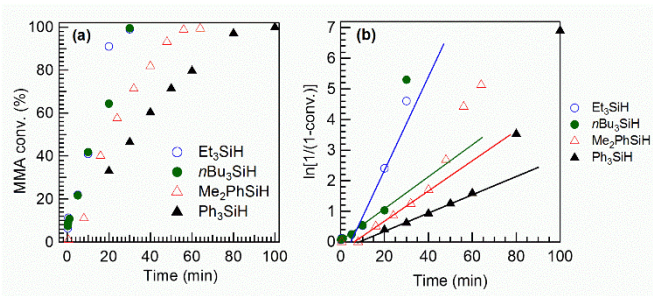

Figure 1. (a) Zero-order plots (MMA conv. *vs.* time) and (b) first-order plots (ln[1/(1-conv.)]) *vs.* time) for the $B(C_6F_5)_3$-catalyzed GTPs of MMA using Et_3SiH, nBu_3SiH, Me_2PhSiH, and Ph_3SiH.

The polymerization kinetics was then investigated at room temperature under the initial $[MMA]_0/[Me_2PhSiH]_0/[B(C_6F_5)_3]_0$ of 50/1/0.5, as shown in Figure 2. For the zero-order plot of conv. *vs.* time (Figure 1a), the conv. increased with the increasing polymerization time and there was no stopping of the polymerization till complete consumption of all the monomer. The first-order plot of ln[1/(1-covn.)] *vs.* time was found to be linear in the low conv. region and showed a self-acceleration phenomenon in the late polymerization stage probably due to the exothermic and viscous effects of the polymerization system.[33] It is worth noting that the induction period time of 6.3 min was observed at the initial polymerization stage in the fitting curve. This induction period could be reasonably assigned to the time required by the 1,4-hydrosilylation of MMA and/or the monomer activation by $B(C_6F_5)_3$ at the very beginning of the polymerization period because the coordination between $B(C_6F_5)_3$ and R_3SiH and that between $B(C_6F_5)_3$ and MMA were reported to be the rate-determining steps for the 1,4-hydrosilylation and polymerization processes, respectively.[34,35] In addition, the $M_{n,SEC}$ of the resulting PMMA in Figure 2b linearly increased with the increasing monomer conversion, while the M_w/M_n value showed a decreasing trend. This feature is one of the characteristics for a living polymerization, suggesting that the present polymerization system is certainly the living one. Each measured $M_{n,SEC}$ was observed to be slightly higher than the calculated value ($M_{n,calcd.}$) and the initiation efficiency estimated by each $M_{n,calcd}/M_{n,SEC}$ was in the range of 78 - 81% except for the earliest polymerization point in Figure 2. Therefore, the higher $M_{n,SEC}$ was probably caused by the slightly low initiation efficiency of this polymerization system. Nevertheless, the fact that the initiation efficiency remained unchanged during the entire polymerization course, on the other hand, indicated that the propagating-ends maintained their livingness once they were formed at the very beginning of polymerization period. The detailed reason for the low initiation efficiency was quite complicated because side reactions, such as the 1,2- and 3,4-hydrosilylation of MMA, and three elementary reactions, such as the 1,4-hydrosilylation, initiation, and propagation reactions, could be considered.

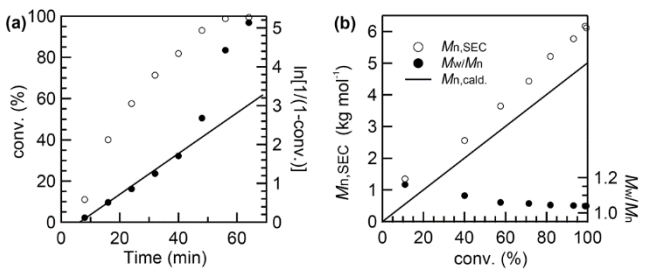

Figure 2. Kinetic plots of the $B(C_6F_5)_3$-catalyzed GTP of MMA using Me_2PhSiH: (a) zero- and first-order plots and (b) the $M_{n,SEC}$ and M_w/M_n dependence of the resulting PMMAs on the conversion.

The living nature of the GTP of MMA was further verified by the chain extension experiments (Figure 3). Subsequent to the completion for the polymerization of 25 *eq.* MMA under the condition of $[MMA]_0/[R_3SiH]_0/[B(C_6F_5)_3]_0$ = 25/1/0.5, another 50 *eq.* MMA was added to examine the propagation of the polymer chain, as to whether or not the polymer chain end kept its living nature. The first-stage polymerization of 25 *eq.* MMA produced a PMMA with the $M_{n,SEC}$ of 3.2 kg mol^{-1} and the M_w/M_n of 1.09. The second-stage polymerization of 50 *eq.* MMA indicated a complete monomer consumption and afforded the polymer product with the $M_{n,SEC}$ of 6.8 kg mol^{-1} and the M_w/M_n of 1.04. The

increase in molar mass was apparently reflected in the SEC profiles as the monomodal SEC trace during the first polymerization stage that was clearly shifted to the high molar-mass region after the completion of the second-stage polymerization, while still maintaining the narrow mono-modal shape. Thus, the chain extension experiments once again implied the living nature of the discussed polymerization system.

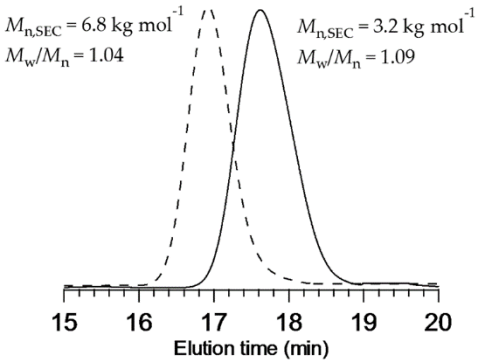

Figure 3. The SEC traces of the PMMA during first-stage polymerization (solid line) and the PMMA during second-stage polymerization (dashed line).

The living characteristics of the $B(C_6F_5)_3$-catalyzed GTP using Me_2PhSiH was used to synthesize well-defined PMMAs with targeted molar masses by varying the initial $[MMA]_0/[Me_2PhSiH]_0$ ratios of 25, 50, 100, 125, and 125. All the monomers were quantitatively consumed for each polymerization and the SEC trace clearly shifted to the high molar-mass region with the increase in the initial $[MMA]_0/[Me_2PhSiH]_0$ ratio, as shown in Figure 4, and all the polymers maintained a narrow polydispersity. The $M_{n,SEC}$s were 3.2, 5.8, 12.2, 12.5, and 17.6 kg mol^{-1}, which was pretty close to the corresponding $M_{n,calcd.}$s of 2.5, 5.0, 10.0, 12.5, and 15.0 kg mol^{-1}, respectively, and all their M_w/M_ns were narrower than 1.10.

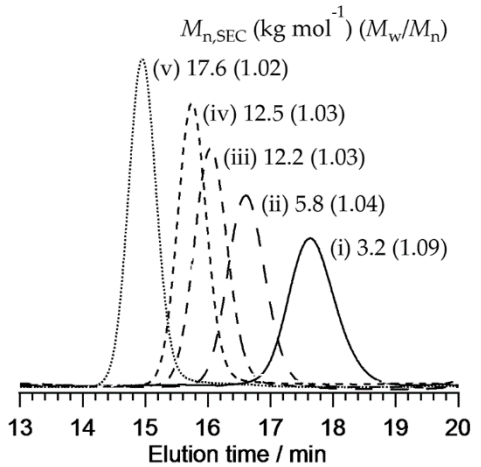

Figure 4. The SEC traces of the PMMAs obtained at various $[MMA]_0/[Me_2PhSiH]_0$ ratios of (i) 25, (ii) 50, (iii) 100, (iv) 125, and (v) 150.

$B(C_6F_5)_3$-catalyzed GTPs of various methacrylate monomers using Me_2PhSiH. In addition to MMA, this GTP method was applied to other methacrylate monomers, such as the alkyl methacrylates of the *n*-propyl (*n*PrMA), *n*-hexyl (*n*HMA), *n*-dodecyl (*n*DMA), 2-ethylhexyl (EHMA), isobutyl (*i*BuMA), cyclohexyl (*c*HMA), and *tert*-butyl (*t*BuMA) ones and functional methacrylates of the allyl (AMA) and 2-(2-methoxyethoxy)ethyl (DEGMA) ones. The polymerizations were carried out with the initial $[monomer]_0/[Me_2PhSiH]_0/[B(C_6F_5)_3]_0$ of 25/1/0.5 and their results are summarized in Table 3. For the GTPs of the alkyl methacrylates, namely, the polymerizations of *n*PrMA, *n*HMA, *n*DMA, EHMA, and *i*BuMA, which possess primary alkyl substituents, completed within 1 h and the obtained $M_{n,SEC}$s were 4.6, 6.4, 6.4, 5.6, and 4.4 kg mol^{-1} for their corresponding polymer products, which was in approximate agreement with the related $M_{n,calcd.}$s of 3.2, 4.3, 6.4, 5.0, and 3.6 kg mol^{-1}, respectively. On the contrary, the polymerization of *c*HMA as a secondary alkyl ester obviously required the long time of 2.7 h, and that of *t*BuMA as a tertiary alkyl ester hardly proceeded. Figure S2 shows the kinetic studies of the GTPs of MMA, *n*HMA, EHMA, and *c*HMA at the $[monomer]_0/[R_3SiH]_0/[B(C_6F_5)_3]_0$ ratio of 50/1/0.5 in CH_2Cl_2 at room temperature. Interestingly, MMA, *n*HMA, and EHMA as primary alkyl esters showed almost the same polymerization behavior and had similar k_p values of ca. 0.05 min^{-1} (Table S1) regardless of the length of the alkyl substituents. In contrast, *c*HMA apparently had a lower polymerization rate (k_p = 0.0184 min^{-1}) than the others (Figure S2), which could be due to the increase in the steric hindrance at the secondary *c*H group. The reason for no polymerization of *t*BuMA was attributed to the cleavage of the *t*Bu-O bond by the strong acidity of $B(C_6F_5)_3$, which, on the contrary, deactivated $B(C_6F_5)_3$. For the GTPs of the functional methacrylates of AMA and DEGMA, the polymerizations ceased after the polymerization time of 18 h, and the monomer conversions were as low as 6.7% for AMA and 19.8% for DEGMA. We attributed this termination to the possible deactivation of the Lewis acid of $B(C_6F_5)_3$ by the more hydrophilic allyl group in AMA and the ether group in DEGMA than that of the carbonyl moiety, which led to no monomer activation and the stopping of the polymerization after a certain period of polymerization. Therefore, the chemical structure of the substituent had a crucial effect on the polymerization rate and possibility of the GTPs of the methacrylate monomers using $B(C_6F_5)_3$ and Me_2PhSiH.

Mechanism of $B(C_6F_5)_3$-catalyzed group transfer polymerization of MMA using Me_2PhSiH. In order to provide a more profound insight into this polymerization system, the polymerization mechanism was studied based on the ^1H NMR measurement of a polymerization system, control experiments of GTP using Me_2PhSiH and an SKA, and the deuteration experiments of the polymer chain-ends. The ^1H NMR spectra of (a) MMA, (b) Me_2PhSiH, (c) a mixture of MMA, Me_2PhSiH, and $B(C_6F_5)_3$ at a molar ratio of 1/1/0.5, and (d) 1-methoxy-2-methyl-1-dimethylphenylsiloxyprop-1-ene (SKA^{Me_2Ph}) prepared by the reaction of methyl isobutyrate with lithium diisopropylamide (LDA) in $CDCl_3$ are shown in Figure 5 in order to compare each

other to ascertain the *in situ* formation of SKA^{Me2Ph} as the true initiator. In the spectrum of the mixture (Figure 5c), the characteristic proton signals completely disappeared at 6.13 and 5.58, 3.68, and 1.98 ppm due to CH_2=C(CH_3)CO_2CH_3, CH_2=C(CH_3)CO_2CH_3 and CH_2=C(CH_3)CO_2CH_3 and at 4.41 and

Table 3. $B(C_6F_5)_3$-catalyzed GTPs of various methacrylate monomers usi

run	Monomer (M)	time (h)	conv. [b] (%)
6	*n*PrMA	1	>99
7	*n*HMA	1	>99
8	*n*DMA	1	>99
9	EHMA	1	>99
10	*i*BuMA	1	>99
11	*c*HMA	2.7	>99
12	*t*BuMA	72	-
13	AMA	18	6.7
14	DEGMA	18	20

[a] Ar atmosphere; temperature, r.t.; $[monomer]_0$, 1.0 mol L^{-1} in CH_2Cl_2; [M in $CDCl_3$. [c] $M_{n,calcd.} = [M]_0/[Me_2PhSiH]_0 \times$ (conv.) × (M.W. of monomer) standards. (- stands for no data)

5a, 5b, and 5c. On the other hand, the new proton signals appeared at 3.41, 1.47-1.61 due to $(CH_3)_2C$=C(OCH_3)(OSiPh$(CH_3)_2$) and $(CH_3)_2$C=C(OCH_3)(OSiPh$(CH_3)_2$) and at 0.63 ppm due to $(CH_3)_2C$=C(OCH_3)(OSiPh(CH_3)$_2$), respectively, by comparing the spectra of Figures 5c and 5d. After the mixing, both MMA and Me_2PhSiH were completely consumed, strongly indicating that the *in situ* 1,4-hydrosilylation of MMA by Me_2PhSiH perfectly proceeded prior to polymerization when such reaction was performed at a $[MMA]_0/[Me_2PhSiH]_0/[B(C_6F_5)_3]_0$ = 1/1/0.5, and the 1,4-hydrosilylation rate was much higher than that for the propagation of MMA since no oligomer or polymer was produced after the formation of SKA^{Me2Ph}. It has been reported that the 1,4-hydrosilylation of an α-unsaturated ketone using a hydrosilane took place subsequent to the activation reaction of the hydrosilane by $B(C_6F_5)_3$.[34,36] Thus, we also checked the ^1H spectrum of the mixture of $[Me_2PhSiH]_0$ and $[B(C_6F_5)_3]_0$ at the molar ratio of 2:1 in $CDCl_3$ versus that of Me_2PhSiH. Unfortunately, no obvious change in the

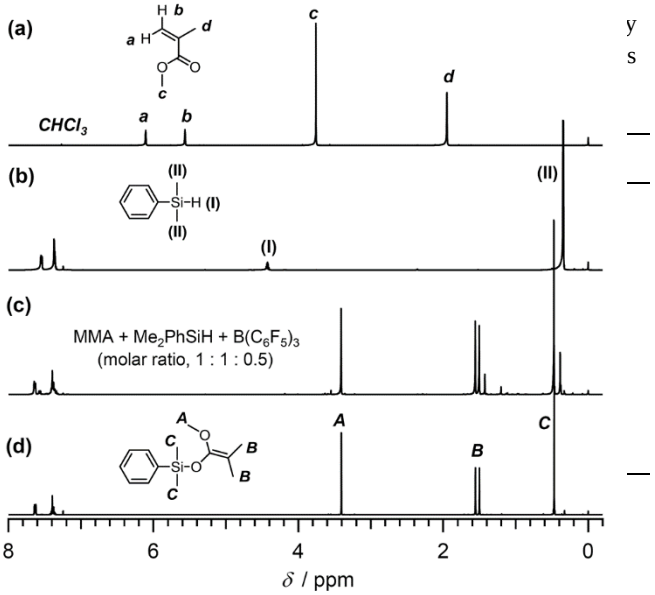

Figure 5. ^1H NMR spectra of (a) MMA, (b) Me_2PhSiH, (c) MMA + Me_2PhSiH + $B(C_6F_5)_3$, and (d) 1-methoxy-2-methyl-1-dimethylphenylsiloxyprop-1-ene (SKA^{Me2Ph}) in $CDCl_3$.

chemical shift was observed because the interaction between Me_2PhSiH and $B(C_6F_5)_3$ was very weak. Nonetheless, based on the facts that mixing Me_2PhSiH, $B(C_6F_5)_3$, and MMA in $CDCl_3$ produced SKA^{Me2Ph}, while mixing Me_2PhSiH and MMA in $CDCl_3$ did not, it is rather clear that $B(C_6F_5)_3$ catalyzed the *in situ* 1,4-hydrosilylation of MMA with Me_2PhSiH.

Table 4. Control $B(C_6F_5)_3$-catalyzed polymerizations of MMA using Me_2PhSiH and SKA^{Me2Ph} [a]

run	$[Me_2PhSiH]_0/[B(C_6F_5)_3]_0$	conv. [b] (%)	$M_{n,SEC}$ [c] (kg mol^{-1})	M_w/M_n [c]
15	0/0.5	0	-	-
16	1/0	0	-	-
17	1/0.5	>99	3.1	1.08
	$[SKA^{Me2Ph}]_0/[B(C_6F_5)_3]_0$			
18	0/0.5	0	-	-
19	1/0	0	-	-
20	1/0.5	>99	3.3	1.08

[a] Ar atmosphere; temperature, r.t.; $[MMA]_0$, 1.0 mol L^{-1} in CH_2Cl_2; $[MMA]_0/[Me_2PhSiH$ or $SKA^{Me2Ph}]_0$, 25. [b] Determined by ^1H NMR in $CDCl_3$. [c] Determined by SEC in THF using PMMA standards.

For the control experiments of the GTPs using Me_2PhSiH or a SKA (Table 4 and Figure S3), the polymerizations of 25 equivalents of MMA were carried out at room temperature in CH_2Cl_2 at the $[Me_2PhSiH]_0/[B(C_6F_5)_3]_0$ ratios of 0/0.5 (run 15), 1/0 (run 16), and 1/0.5 (run 17) and the $[SKA^{Me2Ph}]_0/[B(C_6F_5)_3]_0$ ratio of 0/0.5 (run 18), 1/0 (run 19), and 1/0.5 (run 20). In the cases of the $[Me_2PhSiH]_0/[B(C_6F_5)_3]_0$ of 0/0.5 and the $[SKA^{Me2Ph}]_0/[B(C_6F_5)_3]_0$ of 0/0.5, the polymerizations in absence of Me_2PhSiH as a precursor of the initiator and SKA^{Me2Ph} as a true initiator did not produce any oligomeric and polymeric products,

suggesting that Me_2PhSiH indeed played the role of a potential initiator during the polymerization process and $B(C_6F_5)_3$ could not initiate the polymerization without Me_2PhSiH. In the cases of the $[Me_2PhSiH]_0/[B(C_6F_5)_3]_0$ of 1/0 and the $[SKA^{Me_2Ph}]_0/[B(C_6F_5)_3]_0$ of 1/0, the polymerizations without $B(C_6F_5)_3$ also did not produce any oligomeric or polymeric products, suggesting that $B(C_6F_5)_3$ undoubtedly acted as the catalyst during the polymerization course. In the cases of the $[Me_2PhSiH]_0/[B(C_6F_5)_3]_0$ of 1/0.5 and the $[SKA^{Me_2Ph}]_0/[B(C_6F_5)_3]_0$ of 1/0.5, the polymerizations afforded the targeted polymers as expected. These control experiments led to the conclusion that $B(C_6F_5)_3$ played the role of a dual catalyst for both the 1,4-hydrosilylation and polymerization reactions, and the coexistence of $B(C_6F_5)_3$ and a hydrosilane is dispensable in this GTP system.

Scheme 2. Synthesis of the α,ω-dihydro, α-hydro,ω-deutro, α-deutero,ω-hydro, and α,ω-dideutero poly(methyl methacrylate)s (H-PMMA-H, H-PMMA-D, D-PMMA-H, and D-PMMA-D, respectively) by $B(C_6F_5)_3$-catalyzed GTP of MMA using Me_2PhSiH or Me_2PhSiD as the potential initiator and CH_3OH or CD_3OD as the quenching agent.

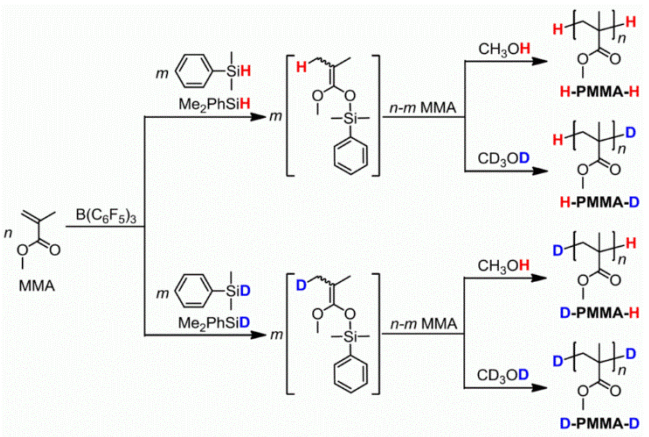

Table 5. $B(C_6F_5)_3$-catalyzed GTP of MMA using Me_2PhSiH or Me_2PhSiD as a potential initiator and CH_3OH or CD_3OD as a terminator [a]

run	Initiation	Termination	$M_{n,SEC}$ [b] (kg mol^{-1})	M_w/M_n [b]	Polymer
17	Me_2PhSiH	CH_3OH	3.1	1.08	H-PMMA-H
21	Me_2PhSiH	CD_3OD	2.9	1.09	H-PMMA-D
22	Me_2PhSiD	CH_3OH	3.2	1.09	D-PMMA-H
23	Me_2PhSiD	CD_3OD	3.4	1.09	D-PMMA-D

[a] Ar atmosphere; $[MMA]_0$, 1.0 mol L^{-1} in CH_2Cl_2; polymerization time, 1 h; temperature, r.t.; $[MMA]_0/[dimethylphenylsilane]_0/[B(C_6F_5)_3]_0$, 25/1/0.5; conv. determined by ^1H NMR in $CDCl_3$, > 99%; $M_{n,calcd.}$, 2.5 kg mol^{-1}. [b] Determined by SEC in THF using PMMA standards.

The deuteration experiments of the polymer chain-ends were further carried out in order to provide direct proof that the initiation reaction started from dimethylphenylsilane, as shown in Scheme 2. Me_2PhSiD was used as a potential initiator for the deuteration at an initiating-end and CD_3OD as a quenching agent (terminator) for that at a terminating-end. A series of four PMMAs with different initiating- and terminating-ends, such as the α,ω-dihydro, α-hydro,ω-deutro, α-deutero,ω-hydro, and α,ω-dideutero PMMAs (H-PMMA-H, H-PMMA-D, D-PMMA-H, and D-PMMA-D, respectively), were prepared by combining the use of dimethylphenylsilane of Me_2PhSiH and Me_2PhSiD and methanol of CH_3OH and CD_3OD; their synthetic details are summarized in Table 5. All the polymerizations were carried out in CH_2Cl_2 at room temperature at the $[MMA]_0/[dimethylphenylsilane]_0/[B(C_6F_5)_3]_0$ ratio of 25/1/0.5. All the polymerizations were completed within 1 h and four-type targeted polymers with their $M_{n,SEC}$s around 3.0 kg mol^{-1} and M_w/M_ns less than 1.10 were obtained.

The MALDI-TOF MS spectra in Figure 6 revealed the detailed compositional structures of these products. For each product, only one series of molecular ion peaks was observed in its spectrum and the *m*/*z* interval between any two neighbouring molecular ion peaks was approximately 100.05, which corresponds to the exact molar mass of MMA as a monomer unit. Furthermore, in the expanded MALDI-TOF MS spectra, the observed values of the 25-mer molecular ion peak were 2526.71, 2527.82, 2527.66, and 2528.64 Da for the sodium-cationized H-PMMA-H, H-PMMA-D, D-PMMA-H, and D-PMMA-D, respectively, which fairly matched with their corresponding sodium-cationized 25-mer monoisotopic values of 2526.24, 2527.25, 2527.25, and 2528.26, respectively. These MALDI-TOF MS results strongly supported that the polymerizations using the dimethylphenylsilane/methanol combinations of Me_2PhSiH/CH_3OH, Me_2PhSiH/CD_3OD, Me_2PhSiD/CH_3OH, and Me_2PhSiD/CD_3OD led to the targeted polymer products of H-PMMA-H, H-PMMA-D, D-PMMA-H, and D-PMMA-D, as designed and desired.

The deuterium atom for H-PMMA-D, D-PMMA-H, and D-PMMA-D was further confirmed by ^2H NMR measurements in $CHCl_3$ at room temperature, as shown in Figure 7. There are no deuterium signals in the ^2H NMR spectrum of H-PMMA-H, as shown in Figure 7a, because no deuterated compounds were used. For the PMMA of run 21, the deuterium signal from the methine group at the terminating-end was observed at 2.38 ppm, while that due to the methyl deuterium at the initiating-end was not observed at 1.20 ppm, as shown in Figure 7b. For the PMMA of run 22, the observed deuterium signal was just the opposite to those of run 21, *i.e.*, the deuterium signal from the methyl at the initiating-end was observed at 1.20 ppm, while that due to the methine deuterium at the terminating-end was not observed at 2.38 ppm. These results were perfectly consistent with the designed structures of H-PMMA-D and D-PMMA-H when using the dimethylphenylsilane/methanol combinations of Me_2PhSiH/CD_3OD and Me_2PhSiD/CH_3OH, respectively. For the PMMA obtained from run 23, the characteristic signals due to the deuterium of the methyl group at the initiating-end and that of the methane group at the terminating-end were simultaneously observed at 1.20 and 2.38 ppm, respectively, suggesting that the D-PMMA-D structure was definitely formed. These results strongly indicated that the hydrogen of Me_2PhSiH or the deuterium of Me_2PhSiD was indeed introduced into the initiating-end of the

PMMA prepared by the $B(C_6F_5)_3$-catalyzed GTP using Me_2PhSiH or Me_2PhSiD. In addition, the perfect deuteration at the terminating-end using CD_3OD indicated that only the propagation reaction and no side reactions, such as chain transfer and backbiting reactions, occurred during the entire polymerization.

Based on the mechanistic study of the 1,4-hydrosilylation of an α-unsaturated ketone[34,36] and the normally accepted mechanism of

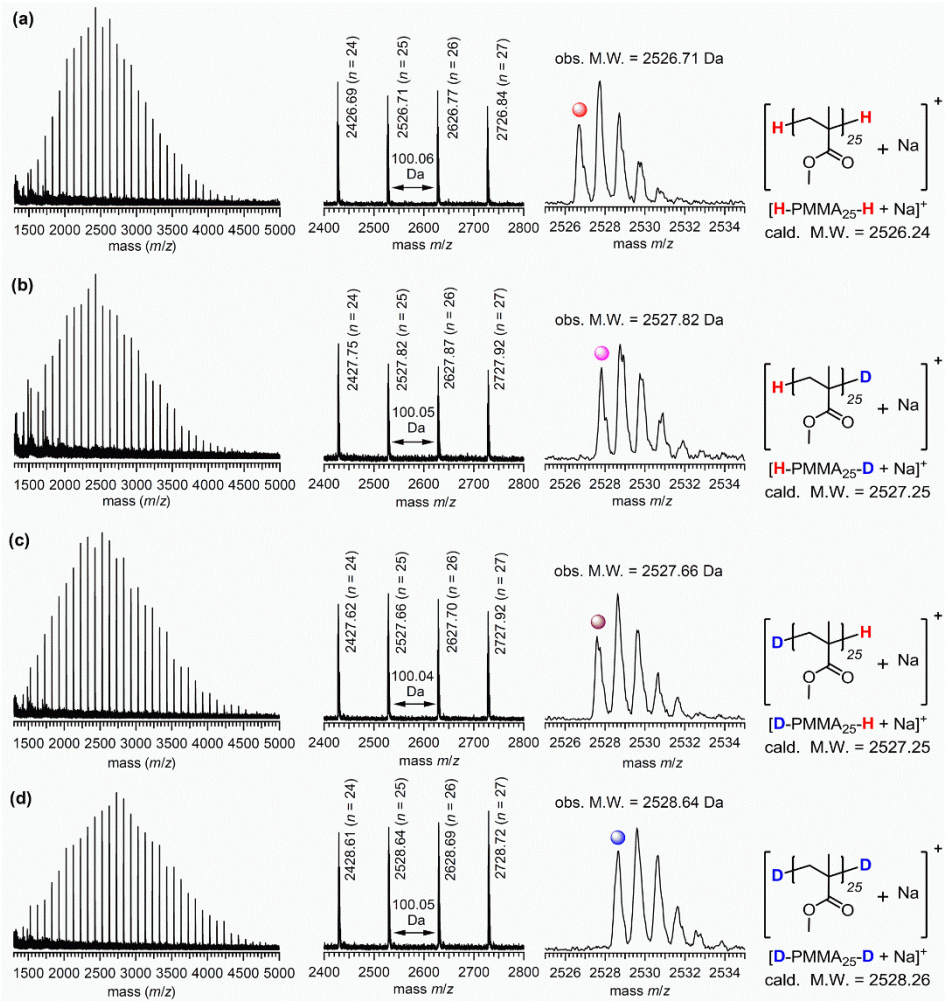

Figure 6. Normal and expanded MALDI-TOF MS spectra in reflector mode of (a) H-PMMA-H (run 17), (b) H-PMMA-D (run 21), (c) D-PMMA-H (run 22), and (d) D-PMMA-D (run 23).

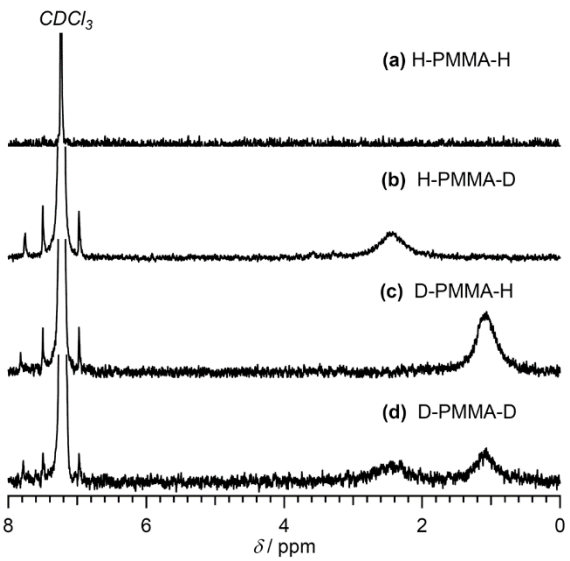

Figure 7. ^2H NMR spectra of (a) H-PMMA-H (run 17), (b) H-PMMA-D (run 21), (c) D-PMMA-H (run 22), and (d) D-PMMA-D (run 23) in $CHCl_3$.

the Lewis acid-catalyzed GTP, we now proposed a plausible mechanism for the $B(C_6F_5)_3$-catalyzed GTP of MMA using a hydrosilane, as shown in Scheme 3. Four elementary reactions are involved during the entire polymerization including (A) activation of the hydrosilane, (B) 1,4-hydrosilylation of MMA to produce the true initiator of SKA^{Me_2Ph} and release of the catalyst, (C) monomer activation by $B(C_6F_5)_3$, and (D) initiation and propagation reactions. We assumed step A, which was reported by Pries et al.[34,36] Step B proceeded very fast and was completed prior to step D as confirmed by the ^1H NMR measurements in Figure 5. Step C seems to be the rate-determining step because steps A, B, and D

were quite fast.[35] The coordination of $B(C_6F_5)$ to the carbonyl group of MMA was not clearly observed by comparing the ^1H NMR spectra of MMA and the mixture of MMA and $B(C_6F_5)_3$ in $CDCl_3$ because no obvious change in the chemical shift was seen due to the activation of MMA by $B(C_6F_5)_3$. This seems once again to support that step C was relatively slower than the other steps. Step D was widely accepted for the Lewis acid-catalyzed GTP. Therefore, we definitely proposed the new GTP mechanism through the *in situ* formation of silyl ketene acetals by the 1,4-hydrosilylation of methacrylate monomers.

Scheme 3. A proposed mechanism for the $B(C_6F_5)_3$-catalyzed GTP of MMA using Me_2PhSiH.

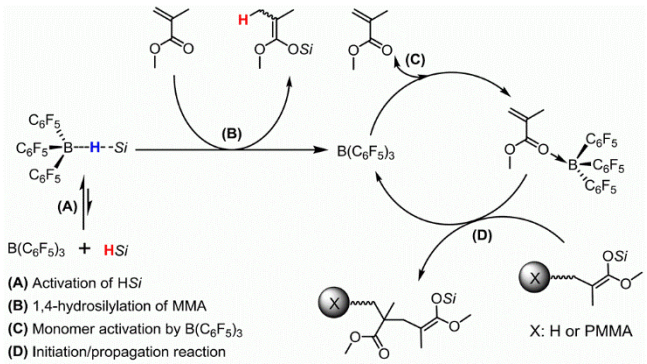

Conclusion

We established the convenient GTP methodology of MMA using Me_2PhSiH and $B(C_6F_5)_3$, in which the direct use of typically employed silyl ketene acteals was avoided. The bulkiness of the used hydrosilane was found to have a significant effect on the polymerization control and moderately bulky hydrosilanes, such as Me_2PhSiH and n-Bu_3SiH, were suitable for the molar-mass control. The $B(C_6F_5)_3$-catalyzed GTP of MMA using Me_2PhSiH was proven to proceed in a living fashion based on the compositional analyses, kinetic studies, and chain extension experiments, which could be applied to produce PMMAs with the targeted molar masses. In addition, this polymerization method could be applied to primary alkyl methacrylate monomers, while the polymerization rates of the secondary alkyl methacrylates were obviously slower than those of the primary alkyl methacrylates and no polymerization proceeded for the tertiary butyl methacrylate. In addition, $B(C_6F_5)_3$ played the important role as a dual catalyst for both the 1,4-hydrosilylation and propagation reactions, suggesting that $B(C_6F_5)_3$ and hydrosilane are dispensable for the present controlled/living GTP system. Finally, the mechanism for the polymerization coupled with the hydrosilylation and Mukaiyama-Michael reactions has been intensively investigated in order to provide a profound insight into the new GTP methodology.

Acknowledgment.

This work was financially supported by the MEXT (Japan) program "Strategic Molecular and Materials Chemistry through Innovative Coupling Reactions" of Hokkaido University and the MEXT Grant-in-Aid for Scientific Research on Innovative Areas "Advanced Molecular Transformation by Organocatalysts". S. Kikuchi and K. Takada were partially funded by the JSPS Fellowship for young Scientists.

Notes and references

§ *Frontier Chemistry Center, Faculty of Engineering, Hokkaido University, Sapporo, 060-8628, Japan.*
† *Division of Biotechnology and Macromolecular Chemistry, Faculty of Engineering, Hokkaido University, Sapporo, 060-8628, Japan.*
‡ Graduate School of Chemical Sciences and Engineering, *Hokkaido University, Sapporo, 060-8628, Japan.*

Corresponding author: kakuchi@poly-bm.eng.hokudai.ac.jp

¶ Y.-G. Chen and K. Kitano contributed equally to this paper.

† Electronic Supplementary Information (ESI) available: The data for MALDI-TOF MS of a PMMA with an average degree of polymerization of 50, kinetics study in Figure S1 and Table S1, and control experiments in Figure S3 are available. See DOI: 10.1039/b000000x/

1 O. W. Webster, W. R. Hertler, D. Y. Sogah, W. B. Farnham and T. V. RajanBabu, *J. Am. Chem. Soc.* 1983, **105**, 5706-5708.
2 O. W. Webster, *J. Polym. Sci., Part A, Polym. Chem.* 2000, **38**, 2855-2860.
3 O. W. Webster, *Adv. Polym. Sci.* 2004, **167**, 1-34.
4 W. Schubert and F. Bandermann, *Makromol. Chem.*, 1989, **190**, 2161-2171.
5 W. Schubert, H. D. Sitz and F. Bandermann, *Makromol. Chem.*, 1989, **190**, 2193-2201.
6 D. Y. Sogah, W. R. Hertler, O. W. Webster and G. M. Cohen, *Macromolecules* 1987, **20**, 1473-1488.
7 W. Schubert and F. Bandermann, *Makromol. Chem.*, 1989, **190**, 2721-2726.
8 W. R. Hertler, D. Y. Sogah and O. W. Webster, *Macromolecules* 1984, **17**, 1415-1417.
9 K. Fuchise, Y.-G. Chen, T. Satoh and T. Kakuchi, *Polym. Chem.* 2013, **4**, 4278-4291.
10 J. Raynaud, A. Ciolino, A. Baceiredo, M. Destarac, F. Bonnette, T. Kato, Y. Gnanou and D. Taton, *Angew. Chem. Int. Ed.* 2008, **47**, 5390-5393.
11 M. D. Scholten, J. L. Hedrick and R. M. Waymouth, *Macromolecules* 2008, **41**, 7399-7404.
12 J. Raynaud, N. Liu, Y. Gnanou and D. Taton, *Macromolecules* 2010, **43**, 8853-8861.
13 J. Raynaud, N. Liu, M. Fèvre, Y. Gnanou and D. Taton, *Polym. Chem.* 2011, **2**, 1706-1712.
14 T. Kakuchi, Y.-G. Chen, J. Kitakado, K. Mori, K. Fuchise and T. Satoh, *Macromoecules* 2011, **44**, 4641-4647.
15 Y.-G. Chen, K. Fuchise, S. Kawaguchi, T. Satoh and T. Kakuchi, *Macromolecules* 2011, **44**, 9091-9098.

16 J. C. Hsu, Y.-G. Chen, T. Kakuchi and W. C. Chen, *Macromoecules* 2011, **44**, 5168-5177.
17 M. Fèvre, J. Vignolle, V. Heroguez and D. Taton, *Macromoecules* 2012, **45**, 7711-7718.
18 Y. Zhang and E. Y.-X. Chen, *Macromolecules* 2008, **41**, 36-42.
19 Y. Zhang and E. Y.-X. Chen, *Macromolecules* 2008, **41**, 6353-6360.
20 G. M. Miyake, Y. Zhang and E. Y.-X. Chen, *Macromoelcules* 2010, **43**, 4902-4908.
21 Y. Zhang, L. O. Gustafson and E. Y.-X. Chen, *J. Am. Chem. Soc.* 2011, **133**, 13674-13684.
22 Y. Zhang, F. Lay, P. García-García, B. List, *Chem. Eur. J.*, 2011, **16**, 10462-10473.
23 R. Kakuchi, K. Chiba, K. Fuchise, R. Sakai, T. Satoh and T. Kakuchi, *Macromolecules* 2009, **42**, 8747-8750.
24 K. Fuchise, R. Sakai, T. Satoh, S. Sato, A. Narumi, S. Kawaguchi and T. Kakuchi, *Macromolecules* 2010, **43**, 5589-5594.
25 K. Takada, K. Fuchise, Y.-G. Chen, T. Satoh and T. Kakuchi, *J. Polym. Sci., Part A, Polym. Chem.* 2012, **50**, 3560-3566.
26 K. Fuchise, Y.-G. Chen, K. Takada, T. Satoh and T. Kakuchi, *Macromol. Chem. Phys.*, 2012, **213**, 1604-1611.
27 Y.-G. Chen, K. Takada, K. Fuchise, T. Satoh and T. Kakuchi, *J. Polym. Sci., Part A, Polym. Chem.* 2012, **50**, 3277-3285.
28 K. Takada, T. Ito, K. Kitano, S. Tsuchida, Y. Takagi, Y.-G. Chen, T. Satoh and T. Kakuchi, *Macromoecules* 2015, **48**, 511-519.
29 K. Takada, K. Fuchise, N. Kubota, T. Ito, Y.-G. Chen, T. Satoh and T. Kakuchi, *Macromolecules* 2014, **47**, 5514-5525.
30 Y.-G. Chen, K. Takada, N. Kubota, O. T. Eric, T. Ito, T. Isono, T. Satoh and T. Kakuchi, *Polym. Chem.* 2015, **6**, DOI: 10.1039/C4PY01564A.
31 K. Fuchise, S. Tsuchida, K. Takada, Y.-G. Chen, T. Satoh and T. Kakuchi, *ACS Macro Lett.*, 2014, **3**, 1015-1019.
32 M. Yan, T. Jin, Y. Ishikawa, T. Minato, T. Fujita, L. Y. Chen, M. Bao, N. Asao, M. W. Chen and Y. Yamamoto, *J. Am. Chem. Soc.*, 2012, **134**, 17536-17542.
33 S. Salzinger, B. S. Soller, A. Plikhta, U. B. Seemann, E. Herdtweck and B. Rieger, *J. Am. Chem. Soc.*, 2013, **135**, 13030-13040.
34 D. J. Parks, J. M. Blackwell and W. E. Piers, *J. Org. Chem.*, 2000, **65**, 3090-3098.
35 E. Y.-X. Chen, *Chem. Rev.* 2009, **109**, 5167-5214.
36 D. J. Parks and W. E. Piers, *J. Am. Chem. Soc.*, 1996, **118**, 9440-9441.

For Table of Contents Graphical Abstract Use Only

$B(C_6F_5)_3$-Catalyzed Group Transfer Polymerization of Alkyl Methacrylates with Dimethylphenylsilane through in Situ Formation of Silyl Ketene Acetal by $B(C_6F_5)_3$-Catalyzed 1,4-Hydrosilylation of Methacrylate Monomer

Yougen Chen,[§,¶] *Kodai Kitano,*[‡,¶] *Shinji Tsuchida,*[‡] *Seiya Kikuchi,*[‡] *Kenji Takada,*[‡] *Toshifumi Satoh,*[‡†] *and Toyoji Kakuchi*[§‡†]*

The $B(C_6F_5)_3$-catalyzed group transfer polymerization (GTP) of alkyl methacrylates using hydrosilane and its polymerization mechanism have been studied in this study.